PHYSICAL REVIEW B **80**, 201408(R) (2009)

Phonon localization and thermal rectification in asymmetric harmonic chains using a nonequilibrium Green's function formalism

Patrick E. Hopkins* and Justin R. Serrano
Sandia National Laboratories, P.O. Box 5800, Albuquerque, New Mexico 87185-0346, USA
(Received 22 September 2009; published 24 November 2009)

Thermal transport across one-dimensional atomic chains is studied using a harmonic nonequilibrium Green's function formalism in the ballistic phonon transport regime. Introducing a mass impurity in the chain and mass loading in the thermal contacts leads to interference of phonon waves, which can be manipulated by varying the magnitude of the loading. This shows that thermal rectification is tunable in a completely harmonic system.

DOI: 10.1103/PhysRevB.80.201408 PACS number(s): 63.22.−m, 44.10.+i, 63.20.kp

Atomistic control in nanostructures has enabled key studies of thermal transport that have demonstrated the potential for phonon control and manipulation in thermal devices. The recent experimental realization[1] of a thermal rectifier mass graded nanotube has been accompanied by several studies in anharmonic one-dimensional (1D) atomic chains in an attempt to understand the origin[2–4] and extent of applicability[5,6] of thermal rectification (i.e., asymmetric heat conduction where heat flows "easier" in one direction than it does in the opposite direction). Recent work examining thermal transport in harmonic chains in the diffuse thermal regime did not exhibit thermal rectification.[7] In this Rapid Communication, we examine thermal transport in asymmetric harmonic chains in the ballistic phonon transport regime with a nonequilibrium Green's function (NEGF) formalism and demonstrate evidence of thermal rectification from phonon-scattering events stemming from phonon wave interference that parallels photon interference in an asymmetric Fabry-Pérot interferometer. We attribute the rectification observed in the asymmetric harmonic chains to localized modes that are unable to propagate the length of the chain before escaping to into the thermal reservoirs, similar to the gradons discussed in by Xiao *et al.*[8]

Our model of the 1D harmonic chain, based on the NEGF formalism[9] for phonons,[10–14] is separated into three regions, as shown in Fig. 1(a). The left and right contact regions, treated as semi-infinite, impose boundary conditions on the N-atom channel region, in which the thermal transport is studied. The left and right contacts impose inflow and outflow in the channel, Σ_{in} and Σ_{out}, which are the self energies of the left or right contacts,[9] depending on the direction of the thermal current, and are related to the harmonic transport in the contacts and the connection at the channel-contact interface. The harmonic spring constants, K_i in the channel, are related to the harmonic forces between the masses, M_i, in the channel. The Green's function of the channel is given by[9] $\tilde{G}=[\tilde{M}\omega^2-\tilde{K}-\tilde{\Sigma}_{\text{in}}-\tilde{\Sigma}_{\text{out}}]^{-1}$ where $\tilde{M}$ is a diagonal matrix of the masses in the channel, ω is the phonon angular frequency, and $\tilde{K}$ is a tridiagonal matrix of spring constants, where the main diagonal represents the restoring force of the atom in position i and the two off-diagonal terms represent the forces from the atoms in position $i-1$ and $i+1$ acting on atom in position i. The left and right contacts cause energy-level broadening at the contact-channel interface described by $\Gamma_{\text{in/out}}=i[\tilde{\Sigma}_{\text{in/out}}-\tilde{\Sigma}^{\dagger}_{\text{in/out}}]$. Given the Green's function of the channel and the level broadening due to the contacts, the thermal transmission across the 1D channel is given by[9] $\tau=\text{Trace}[\tilde{\Gamma}_{\text{in}}\tilde{G}\tilde{\Gamma}_{\text{out}}\tilde{G}^{\dagger}]$.

The Hamiltonian of the 1D harmonic chain in this work is given by

$$H=\frac{1}{2}\tilde{u}_t^{\dagger}\tilde{M}\tilde{u}_t+\frac{1}{2}\tilde{u}^{\dagger}\tilde{K}\tilde{u}. \tag{1}$$

where $\tilde{u}$ is a matrix describing the displacements of the atoms in the channel and $\tilde{u}_t$ is the time derivative of the displacement matrix. As described by Zhang *et al.*,[13] for a harmonic Hamiltonian in the form of Eq. (1) the thermal conductance through the atomic chain is given by

$$\lambda=\frac{\hbar}{2\pi}\int_0^{\omega_c}\omega\tau\frac{\partial f}{\partial T}d\omega \tag{2}$$

where T is the temperature of the channel, f is the Bose-Einstein distribution function, and τ is the thermal transmission coefficient across the channel, as previously mentioned. The thermal conductance in this Green's function approach is derived from the Landauer formalism, and is derived in detail in the references.[9,10,13,15] The temperature dependency of Eq. (2) comes from the Landauer approach[16] where each semi-infinite contact is prescribed a different temperature causing a net flux between the contacts; the temperature dependencies of phonon populations in the contacts gives rise

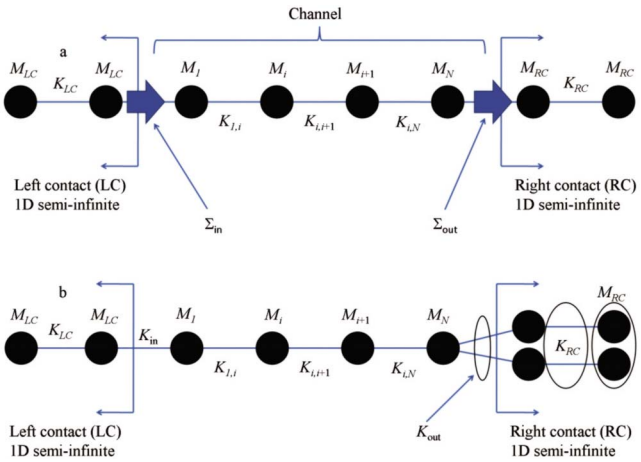

FIG. 1. (Color online) Schematic of (a) atomic chain with important regions identified for NEGF development and (b) atomic chain with mass loading in right contact. We refer to a contact that is more than a single atomic chain as a "mass-loaded contact," such as the right contact depicted in (b).

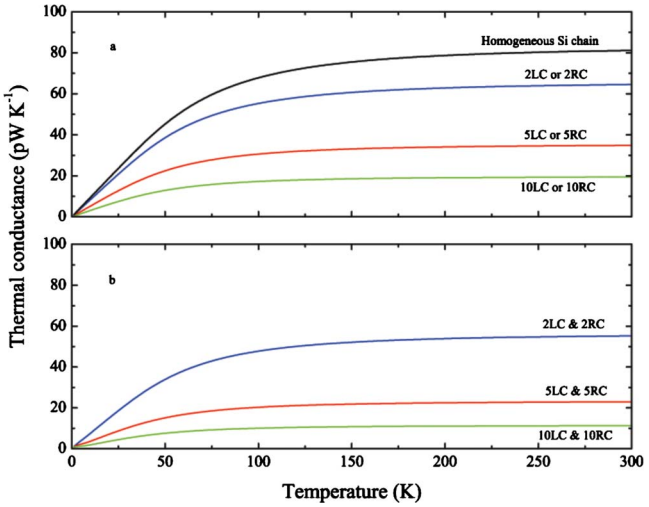

FIG. 2. (Color online) Thermal conductance of a homogeneous 10 atom channel under various (a) asymmetric and (b) symmetric mass loadings of the contacts. The conductance of a homogeneous Si chain (no mass loading in the contacts) is shown in (a) for comparison. In all cases shown in (a) and (b), no rectification is observed even when there is asymmetric mass loading of the contacts.

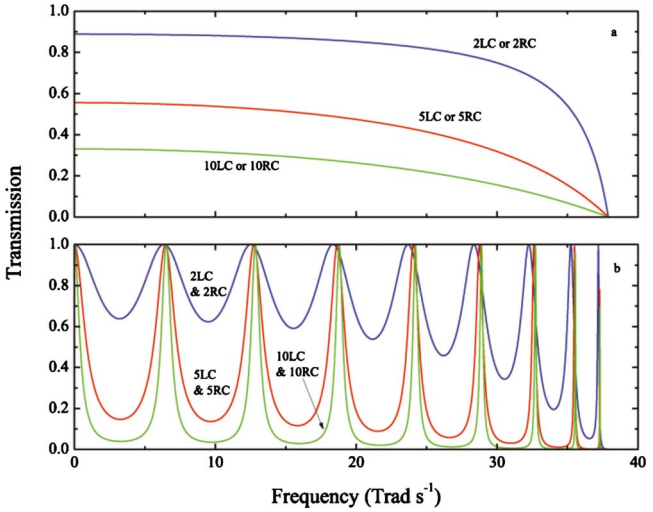

FIG. 3. (Color online) Channel thermal transmissions for the thermal conductance calculations shown in Fig. 2. With symmetric mass loading, the transmission spectra exhibits Fabry-Pérot-like oscillations resulting from interference of the phonon waves that are reflecting off the contact-channel interfaces.

to a net flux across the channel. The thermal conductance, Eq. (2), is evaluated in the limit of an infinitesimally small temperature difference. Evaluation of Eq. (2) for the various atomic chains of interest requires knowledge of the mass at each point in the atomic chain and the spring constants between each mass. The masses at each point are taken as some multiple of the atomic mass of Si, $M=4.7\times10^{-26}$ kg. The spring constants are calculated from the second derivative of the harmonic Harrison potential,[17] which, for a 1D chain, is given by $K=3ac_{11}/16$, where a and c_{11} are the interatomic spacing and elastic constant for Si, taken as 0.543 nm and 16.57×10^{10} N m^{-2}, respectively, giving $K=16.87$ N m^{-1}. For this harmonic chain, the maximum frequency of vibration is $\omega_c=2\sqrt{K/M}$. With M and K of the left and right contacts, the self-energies of each of the contacts can be calculated by

$$\Sigma_{\text{in/out}} = -K_{\text{in/out}} \exp\left[2i \sin^{-1}\left(\frac{\omega}{\omega_c}\right)\right] \tag{3}$$

where $K_{\text{in/out}}$ is the spring constant at the channel-contact interface. This form of the self energy is derived in detail for phonons propagating in a atomic chain by Hopkins *et al.*[10]

Figure 2(a) shows the thermal conductance for a Si chain, assuming the contacts and channels are all Si atoms with mass M and spring constant K. The spring constants at the channel-contact interface are also K since the channel and contacts are all single Si atoms. Figure 2(a) also shows the conductance for a 10 atom chain where the geometry of the left contact and channel are single Si atoms and the right contact is twice as massive. This geometry, shown in Fig. 1(b), is simulated as a chain that has a mass-loaded thermal contact with two masses on the right contact [we refer to a contact that is more than a single atomic chain as a "mass-loaded contact," such as the right contact depicted in Fig. 1(b)]. The two masses are treated as independent and are not coupled by any transverse forces, such that the mass at the right contact is $2M$ and the springs joining it to the channel are in parallel with an effective spring constant of $2K$. This scenario is denoted as 2RC. To simulate a reversal of the thermal current for such asymmetric chains, the contacts are simply reversed. Therefore, 2LC in Fig. 2(a) simulates a left contact with two times mass-loaded properties and a channel and right contact with single mass properties.

The asymmetry in the masses of the contacts leads to a phonon distribution near one contact that is different than the phonon distribution near the other contact. By switching the contacts in the mass asymmetric cases, we simulate switching the thermal current. Considering rectification as a difference in the thermal conductance of the channel that depends on the direction of the thermal current,[18] it becomes clear from Fig. 2(a) that these mass-loaded contacts do not produce rectification in the 10 atom harmonic chains. For comparison, the same cases for 5LC, 5RC, 10LC, and 10RC were calculated and shown in Fig. 2(a). No rectification is observed in any of the cases shown in Fig. 2(a) of their corresponding thermal transmission spectra, shown in Fig. 3(a); the transmission for the nonmass-loaded homogeneous Si chain is unity (not shown). This is expected, as with a homogeneous chain, both the left and right mass-loaded contact cases result in otherwise identical systems.

Figure 2(b) shows the same scenarios in Fig. 2(a), for the symmetric chain cases where both contacts are loaded with the same mass, i.e., 2LC and 2RC, 5LC and 5RC, and 10LC and 10RC. The thermal transmission spectra for the ten-atom chain scenarios are shown in Fig. 3(b) and exhibit Fabry-Pérot-like oscillations resulting from interference of the phonon waves that are reflecting off the contact-channel interfaces. These oscillations are not observed in the asymmetric mass-loaded cases since one of the contact-channel interfaces is a homogeneous contact and therefore back reflection of the phonon waves was not present at that interface.

By manipulating and localizing the Fabry-Pérot phonon oscillations, thermal rectification can be controlled. This can be accomplished by considering the contact mass-loading

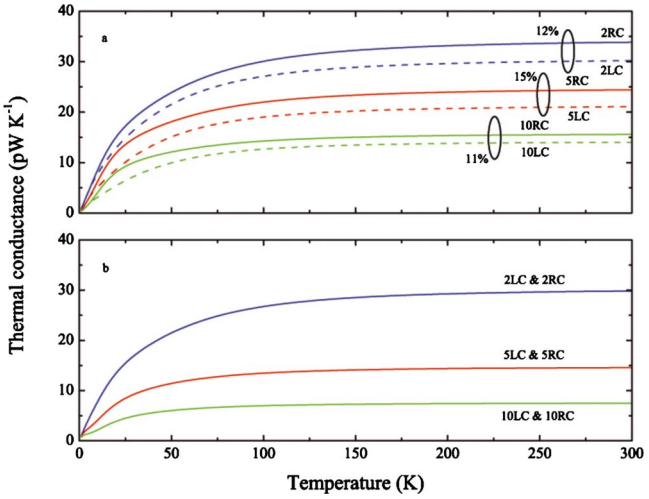

FIG. 4. (Color online) Thermal conductance of a 10 atom channel containing an impurity of mass $2M$ at position 8 under various (a) asymmetric and (b) symmetric mass loadings of the contacts. In the case of asymmetric mass loading of the contacts, the impurity causes asymmetric thermal conductance, creating thermal rectification greater than 10%. Symmetric mass loading of the contacts does not create a directional dependent thermal conductance.

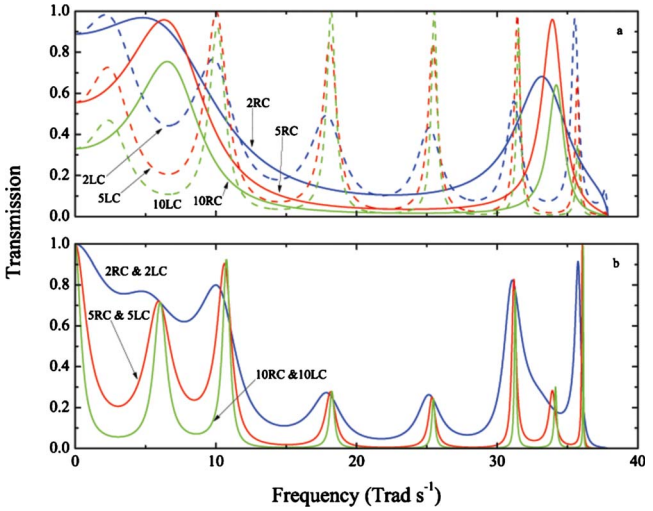

FIG. 5. (Color online) Channel thermal transmissions for the thermal conductance calculations shown in Fig. 4. Broadening of the oscillations between the impurity and the mass-loaded contact when the mass-loaded contact is on the right (solid lines) causes the thermal conductance to be greater than when the mass-enhanced contact is at the left (dashed lines). Note that the transmission spectra is not directionally dependent when the contacts are symmetrically mass loaded even when the channel is asymmetric (b).

cases discussed previously now with an impurity introduced to make the channel region inhomogeneous. In this case, we consider a ten-atom channel with an impurity of mass $2M$ introduced as the eighth atom from the left contact (third atom from the right contact) in the same bonding configuration as shown between the channel and right contact in Fig. 1(b). In this geometry, reversal of the thermal current is accomplished by leaving the mass impurity at position 8 and switching the contacts.

Figure 4 shows the thermal conductances for an inhomogeneous 10 atom chain for the various contact mass-loading scenarios discussed in Fig. 2. Figure 4(a) shows thermal conductance calculations when only one of the contacts is mass loaded and Fig. 4(b) shows the thermal conductance when both contacts are mass loaded. Unlike the previous cases, introduction of the impurity as the eighth atom in the ten-atom chain leads to an asymmetric thermal conductance. Reversing the contacts and channel about the midpoint of the channel (i.e., switching the contacts and moving the mass impurity from position 8 to position 3) or using symmetrically mass-loaded contacts, leads to no evidence of rectification which indicates conservation of the second law. This shows that thermal current is equal in each direction for a given thermal bias, but, when the bias is reversed, the thermal current changes (but is still equal in each direction). This is the definition of thermal rectification.[18] Note in Fig. 4(a) that a larger asymmetry in the mass loading does not correspond to a greater rectification. For example, the largest rectification is observed when the asymmetric mass-loading ratio is 5 (that is, one contact is five times "heavier" than the other) indicating that there is some critical parameter related to the asymmetric mass loading and the mass of the impurity (i.e., the asymmetry in the channel).

This phenomenon is explained by examining the thermal transmission through the channels for each of these cases, as shown in Fig. 5. Figure 5(a) compares the thermal transmission spectra for the cases in Fig. 4(a). When the impurity is far from the mass-loaded contact (i.e., when the mass-loaded contact is on the left), sharp Fabry-Pérot-type oscillations are observed (dashed lines). The waves launched into the channel from the mass-loaded contact on the left experience multiple reflections in the channel between the left contact and the impurity atom. This causes significant destructive interference leaving only very sharp, narrow Fabry-Pérot peaks. However, in the case when the impurity is close to the mass-loaded contact (i.e., when the mass-loaded contact is on the right), the waves launched from the left (nonmass-loaded contact) do not experience multiple reflections between the impurity and the left contact-channel interface since the left contact and channel are the same material (solid lines). This reduces the amount of destructive interference of the right-traveling in-flow leading to broadening of the multiple reflections between the atom 8 impurity and the right mass-loaded contact. Even though the multiple reflections between atom 8 and the right mass-loaded contact are less than those between atom 8 and the left mass-loaded contact, the broadening increases the transmission to enhance thermal conductance. These localized vibrations that are affected by Fabry-Pérot-like phonon interference between two mass-enhanced regions of a 1D chain are similar to gradons,[8] and can be used to control phonon thermal conductance. The differences seen in Fig. 4(a) among the different mass loading of the contacts suggest that there is also a dependency between the mass loading of the contacts, and the mass enhancement at the impurity site. Figure 5(b) compares the thermal transmission spectra for the cases in Fig. 4(b). Note that the transmission spectra are not directionally dependent which means there is no thermal rectification. Fabry-Pérot phonon oscillations are still observed in the channel due to the impurity

atom in the channel, but the symmetry of the masses in the contacts means that asymmetric heat conduction is not possible.

As observed in Figs. 4 and 5, the key to thermal rectification during harmonic, ballistic phonon transport is asymmetric mass loading in the contacts and some nonsymmetric phonon scattering event (i.e., the channel "impurity" atom). The asymmetric mass-loaded contacts in our study cause the contacts to have different self energies, meaning that the imposed wave interacts differently with each contact. This is similar to the conclusion reached recently examining thermal rectification in structures with geometrically asymmetric phonon-scattering sites, where the condition for rectification is that the phonon baths driving conductance must be at different temperatures and perturbed from equilibrium.[19] However, this study treats the phonons as particles and the scattering sites scatter the phonon particles classically leading to phonon rectification that is only realized when there is a substantial temperature gradient. We show that a large temperature gradient is not necessary for rectification of phonon conductance if phonon transport is in the wave regime. This is applicable in low dimensional nanostructure applications when characteristic lengths are less than the phonon mean-free paths.

Further insight into the origin of thermal rectification during harmonic, ballistic phonon transport is gathered by examining the rectification as a function of impurity position. Figure 6 shows the thermal rectification percentage, which here is defined as $|\lambda_{RC/LC}-\lambda_{LC/RC}|/\lambda_{LC/RC}$ where the subscripts represent which contact is mass loaded, as a function of impurity position at 300 K for the cases described in Fig. 4(a). There are two main features of the trends in Fig. 6 that are important for rectification. First off, the length of the "Fabry-Pérot phonon cavity" drastically affects the rectification. Secondly, the degree of mass loading has a complex relationship on the rectification, where the rectification is extremely sensitive to impurity position with a large asymmetry in the mass loading with the sensitivity decreasing as the mass loading becomes more symmetric.

In summary, phonon thermal conductance in harmonic chains is studied with a nonequilibrium Green's function formalism. In atomic chains with different contacts, introducing a mass impurity in the atomic chain causes asymmetric thermal transport creating thermal rectification assuming purely harmonic, ballistic transport. This is due to phonon wave interference similar to Fabry-Pérot interference. This type of phonon wave and thermal transport control gives a straight forward way to design thermal switches, amplifiers, and thermal memory devices[5,6] through controlled impurity growth creating multiple reflections between the impurity and the thermal source or sink, effectively creating Fabry-Pérot phonon interference filters.

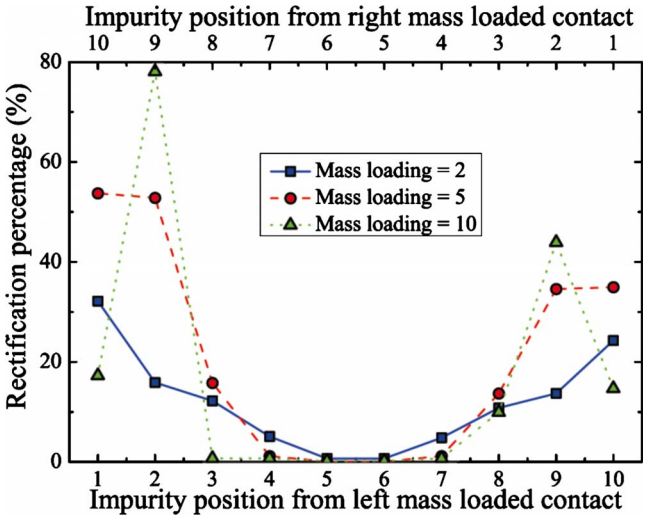

FIG. 6. (Color online) Thermal rectification percentage as a function of impurity position at 300 K for the cases described in Fig. 4. The length of the "Fabry-Pérot phonon cavity" drastically affects the rectification and the rectification percentage is extremely sensitive to impurity position.

P.E.H. is grateful for support from the LDRD program office through Sandia National Laboratories. The authors would like to thank Chris Dames at U.C. Riverside for insightful discussions on thermal rectification. Sandia is a multiprogram laboratory operated by Sandia Corporation, a Lockheed-Martin Co., for the United States Department of Energy's National Nuclear Security Administration under Contract No. DE-AC04-94AL85000.

*Author to whom correspondence should be addressed; pehopki@sandia.gov

[1] C. W. Chang *et al.*, Science **314**, 1121 (2006).
[2] N. Yang *et al.*, Phys. Rev. B **76**, 020301(R) (2007).
[3] Yong Xu *et al.*, Phys. Rev. B **78**, 224303 (2008).
[4] B. Hu *et al.*, Phys. Rev. Lett. **97**, 124302 (2006).
[5] B. Li *et al.*, Appl. Phys. Lett. **88**, 143501 (2006).
[6] L. Wang and B. Li, Phys. Rev. Lett. **101**, 267203 (2008).
[7] D. Segal, Phys. Rev. E **79**, 012103 (2009).
[8] J. J. Xiao *et al.*, Phys. Rev. B **73**, 054201 (2006).
[9] S. Datta, *Quantum Transport: Atom to Transistor* (Cambridge Univeristy Press, Cambridge, 2006).
[10] Patrick E. Hopkins *et al.*, J. Appl. Phys. **106**, 063503 (2009).
[11] N. Mingo and L. Yang, Phys. Rev. B **68**, 245406 (2003).
[12] W. Zhang *et al.*, ASME J. Heat Transfer **129**, 483 (2007).
[13] W. Zhang *et al.*, Numer. Heat Transfer, Part B **51**, 333 (2007).
[14] W. Zhang *et al.*, Phys. Rev. B **76**, 195429 (2007).
[15] S. Datta, *Electronic Transport in Mesoscopic Systems* (Cambridge University Press, Cambridge, 1995).
[16] Y. Imry and R. Landauer, Rev. Mod. Phys. **71**, S306 (1999).
[17] W. A. Harrison, *Electronic Structure and the Properties of Solids: The Physics of the Chemical Bond* (W. H. Freeman and Company, San Francisco, 1980).
[18] C. Dames, ASME J. Heat Transfer **131**, 061301 (2009).
[19] J. N. Miller *et al.*, *Proceedings of the ASME 2009 Heat Transfer Summer Conference, San Francisco, 2009* (ASME, New York, 2009), Vol. HT2009, p. 88488.